Supplementary material (ESI) for Journal of Materials Chemistry

Gold-layered Calcium Phosphate Plasmonic Resonants for Localized Photothermal Treatment of Human Epithelial Cancer

Jinyoung Kang, Jaemoon Yang, Jaewon Lee, Seung Jae Oh, Seyoung Moon, Hong Jae Lee, Sangcheon Lee, Joo-Hiuk Son, Donghyun Kim, Kwangyeol Lee, Jin-Suck Suh, Yong-Min Huh* and Seungjoo Haam*

Materials: Calcium hydroxide, phosphoric acid, tetrachloroaurate (III) trihydrate, tetrakis (hydroxymethyl) phosphonium chloride solution, sodium hydroxide, 3-aminopropyltrimethoxysilane, potassium carbonate and formaldehyde were purchased from Sigma-Aldrich Chemicals and phosphate buffered saline (PBS, 10 mM, pH7.4) was purchased from Hyclone and used without further purification. Human immunoglobulin G (IgG) as an irrelevant antibody and FITC-labeled goat anti-human IgG were purchased from ZyMaxTM. Erbitux® was purchased from Roche Pharmacuetical Ltd. Sephacryl S-300 and calcein AM were purchased from Amersham Biosciences and Molecular Probes, respectively.

Synthesis of calcium phosphate nanoparticles (CPNs): Calcium phosphate nanoparticles (CPNs) were synthesized by a chemical precipitation and hydrothermal technique according to a previously published protocol with some modifications.[1] An aqueous solution of phosphoric acid (0.3 M, 300 mL) was added to a vigorously stirred aqueous solution of calcium hydroxide (0.25 M, 625 mL) in a dropwise manner at a rate of 1 mL/min at 60°C. After completion of the phosphoric acid addition, the pH of the suspension was adjusted to pH 7.0. After aging, CPNs were purified and collected by repeated washing with distilled water and centrifugation at 2,500 rpm for 20 minutes (repeated 5 times). The final product of CPNs was obtained by freeze-drying.

Synthesis of calcium phosphate-gold nanocomposites: Gold nanoparticles (GNPs, ~2 nm) were prepared by the reduction of tetrachlorolaurate (III) trihydrate (2 mL of 1.0 wt%) in the presence of a tetrakis (hydroxymethyl) phosphonium chloride solution (12 μL) and sodium hydroxide (0.5 mL of 1 M) solution as a reducing agent for 7 minutes at room temperature. The surface of CPNs was modified by self-assembly of 3-aminopropyltrimethoxysilane (5 μL) and CPNs (40 mg) in 5 mL of distilled water at 70^{o}C for 3 hours. The aminated CPNs were purified by centrifugation and re-dispersed in distilled water (0.5 mL). X-ray photoelectron spectroscopy (XPS) was used to confirm the synthesis of aminated CPNs. Aminated CPNs (40 mg) were stirred with an excess of GNPs (7×10^{14} particles/5 mL). The amine group at CPN surface was used as an attachment site for binding of colloidal GNPs, which then served as nucleation sites for further growth by reduction of gold salts using formaldehyde. This consequently led to the formation of a continuous and reticular gold layer. The gold salts solution was prepared by

adding potassium carbonate (25 mg) into tetrachlroloaurate (III) trihydrate (50 mL of 0.02 wt%). Two hundred μL of CPNs-GNPs solution was mixed with the gold salts solution (4 mL) and formaldehyde (80 μL) for 5 minutes. After a 2-fold reduction of gold on CPN-GNPs, CPGNs were formed and purified by repeated washing with distilled water and centrifugation at 15,000 rpm for 20 minutes (repeated 5 times).

Degradation test: The synthesized CPNs can be degraded in an acidic environment according to the following reaction (eq 1).[2] To evaluate the degradation ratio of CPNs, CPNs (4 mg) was immersed in various range of pH solution (5 mL; pH 3, 4, 5, 6 and 7) for 24 hours and transmittance was measured using UV-Vis spectroscopy at 240 nm (Figure S7). Furthermore, the amount of released calcium ions from CPGNs was investigated by inductively coupled plasma mass spectrometry (ICP-MS) at various pH conditions (pH 4, 5 and 7.4). CPGNs (5 mg/mL, 5 mL) was immersed in at each solution for 24 hours and treated with aqua regia which is 3 : 1 mixture of HCl : HNO_3, and evaporated overnight at 110°C and 4 mL of distiled water was added for measuring using ICP-MS. In Figure 1c, relative degradation ratios were calculated using the ratio of calcium ion at pH 4 or 5 to calcium ion at pH 7.4. To confirm change of plasmon peaks during CPGNs degradation, on the other hands, UV-Vis absorption spectra of CPGNs at various pH conditions (pH 3, 4, 5, 6 and 7.4) were analyzed after 120 hours.

$$Ca_{10}(PO_4)_6(OH)_2 + 2H^+ \leftrightarrow 10Ca^{2+} + 6PO_4^{3-} + 2H_2O \quad \text{(eq 1)}$$

Simulation of the extinction spectra of CPNGs: For theoretical analysis of the extinction spectra, a Mie calculation of inhomogeneous ellipsoids was conducted, assuming smooth particle geometry. The surface of the particle is described as:

$$\begin{aligned}
&\frac{x^2}{a_{(i,o)}^2+\xi}+\frac{y^2}{b_{(i,o)}^2+\xi}+\frac{z^2}{c_{(i,o)}^2+\xi}=1, \quad -c_{(i,o)}^2<\xi<\infty \\
&\frac{x^2}{a_{(i,o)}^2+\eta}+\frac{y^2}{b_{(i,o)}^2+\eta}+\frac{z^2}{c_{(i,o)}^2+\eta}=1, \quad -b_{(i,o)}^2<\eta<\infty \\
&\frac{x^2}{a_{(i,o)}^2+\zeta}+\frac{y^2}{b_{(i,o)}^2+\zeta}+\frac{z^2}{c_{(i,o)}^2+\zeta}=1, \quad -a_{(i,o)}^2<\zeta<\infty,
\end{aligned} \quad (2)$$

where a, b and c with subscripts i and o correspond to the inner and outer radii of the x, y, and z axis, respectively, and ξ, η and ζ are derived from the ellipsoidal coordinates. Note in this case that $b = c \leq a$, which corresponds to a prolate ellipsoid with a principle axis coinciding with the x axis. To obtain an extinction cross-section of the particles in response to the field in the x, y and z-axes, the polarizability, $\alpha_{(x, y, z)}$ in each axis was first calculated as:

$$\alpha_{(x,y,z)} = \frac{\upsilon((\varepsilon_2 - \varepsilon_m)[\varepsilon_2 + (\varepsilon_1 - \varepsilon_2)(L^i_{(x,y,z)} - fL^o_{(x,y,z)})] + f\varepsilon_2(\varepsilon_1 - \varepsilon_2)}{[\varepsilon_2 + (\varepsilon_1 - \varepsilon_2)(L^i_{(x,y,z)} - fL^o_{(x,y,z)})][\varepsilon_m + (\varepsilon_2 - \varepsilon_m)L^o_{(x,y,z)}] + fL^o_{(x,y,z)}\varepsilon_2(\varepsilon_1 - \varepsilon_2)}, \quad (3)$$

where the eccentricities of the inner (superscripted *i*) and outer (superscripted *o*) ellipsoids (L_x, L_y *and* L_z) are defined as:

$$L_x^{(i,o)} = \frac{a_{(i,o)}b_{(i,o)}c_{(i,o)}}{2}\int_0^\infty \frac{dq}{(a^2_{(i,o)} + q)F_{(i,o)}(q)}$$

$$L_y^{(i,o)} = \frac{a_{(i,o)}b_{(i,o)}c_{(i,o)}}{2}\int_0^\infty \frac{dq}{(b^2_{(i,o)} + q)F_{(i,o)}(q)} \quad (4)$$

$$L_z^{(i,o)} = \frac{a_{(i,o)}b_{(i,o)}c_{(i,o)}}{2}\int_0^\infty \frac{dq}{(c^2_{(i,o)} + q)F_{(i,o)}(q)}, \text{ and}$$

$$F_{(i,o)}(q) = \sqrt{(a^2_{(i,o)} + q)(b^2_{(i,o)} + q)(c^2_{(i,o)} + q)}.$$

In Eq. (3), $\upsilon = 4\pi a_o b_o c_o$ is the volume of the particle, $f = \frac{a_o b_o c_o}{a_i b_i c_i}$ is the volume fraction of the inner ellipsoid, and $\varepsilon_{(1,2,m)}$ is complex dielectric constant of: 1; inner material, 2; outer material, and m; surrounding medium, respectively. From the description of the scattered electric fields, the extinction cross-section, C_{ext} was obtained from the polarizability calculation with the following relationship:

$$C_{ext} = k\,\mathrm{Im}\{\alpha\}, \quad (5)$$

where the wave vector k is defined as $k = 2\pi/\lambda$.

The extinction spectra of three different types of plasmonic core-shell nanoparticles (ellipsoidal CPGNs, spherical CPGNs and spherical silica-gold core-shell structures) were calculated for comparison. The dielectric constants of gold and water were obtained from the experimental measurements and were interpolated in the wavelengths of interest (400 ~ 1,200 nm).[3] The refractive index of CPNs (1.651) and silica nanoparticles (1.460) were assumed to be constant over the range of wavelengths. The major axis (a) and minor axis (b = c) of the ellipsoidal CPNs was 60 nm and 10 nm, respectively. The thickness of gold shell for CPGNs was 10nm for consistence with the experimental data. The both extinction spectra of the spherical CPGNs and silica gold nanoshells (a = b = c = 18.2 nm) were calculated based on the same core volume and gold shell thickness with the ellipsoidal CPGNs. In Figure S6, the ellipsoidal CPGNs exhibited higher extinction spectra at NIR region rather than spherical CPGNs and silica gold nanoshells.

Conjugation of ERB with CPGNs: In order to conjugate ERB (Erbitux®, anti-EGFR antibody) with CPGNs, 2 mg of ERB was mixed with 4 mg of CPGNs in the PBS (pH 7.4, 10 mM) at 4°C.

After 4 hours, ERB-CPGNs were purified with a Sephacryl S-300 column. The quantity of conjugated ERB onto the surface of CPGNs was evaluated by a BCA protein assay (Thermo Fisher Scientific Inc.) and 20 equivalent ERB was conjugated on to CPGNs. Similarly, for control experiments, the irrelevant (IRR) human immunoglobulin G (IgG) antibody was conjugated with CPGNS. The IRR-conjugated CPGNs was synthesized with the same manner as described for ERB-CPGNs.

Cellular affinity test: The epidermoid carcinoma A431 and MCF7 cell lines were obtained from American Tissue Type Culture (ATCC, Rockville, MD) and cultured. Briefly, the cells (1×10^5 cells/mL) were seeded in 100 ϕ Corning culture dishes (10 mL/dish) with Dulbecco's Modified Eagle Medium supplemented with 10% fetal bovine serum (FBS) and 1% antibiotics and incubated at 37 ^oC in a humidified atmosphere composed of 5% CO_2. Fluorescence-activated cell sorting (FACS) analysis was performed to determine the affinity of ERB-CPGNs (1 mg/mL, 200 μL) for A431 and MCF7 cells, respectively. A431 and MCF7 cells were washed with buffer (2 % FBS and 0.02 % NaN_3 in PBS) and then the cells were incubated with ERB-CPGNs and IRR-CPGNs for 1 hour at 4 ^oC, respectively. The temperature was maintained at 4^oC in order to avoid non-specific binding through endocytosis without receptor-mediated uptake. The treated cells were washed three times with an FITC-labeled goat anti-human IgG for 45 minutes at 4^oC in the dark room. Finally, the cells were suspended in 400 μL PBS and stored at 4^oC prior to FACS analysis (Becton Dickinson, Mountain View, California, USA).

Investigation of therapeutic efficacy: A431 and MCF7 cells (4×10^3 cells/well) were incubated in 96-well plates for 24 hours. Target cells were incubated with ERB-MGNCs or IRR-MGNCs (1 mg/mL, 100 μL) at 37^oC. After 4 hours, an equal volume of 10% FBS was added to each of the wells, and the cells were incubated for an additional 72 hours. During exposure to an NIR laser, thermographic data were recorded with an infrared thermal camera (Thermographic System, AXT100) with time intervals of 1 second over a course of 5 minutes, and the temperature of the cells was then calculated from the images using Thermographic System software. After exposure to an NIR laser (820 nm and 25 W/cm^2 for 5 minutes), the cells were incubated for 2 hours at 37^oC. The distribution of live and dead cells after staining with a calcein AM (l μM) was observed using a fluorescence microscope. The therapeutic efficacies were determined by calculating the differences between cell viabilities under treated and non-treated conditions (n=3).

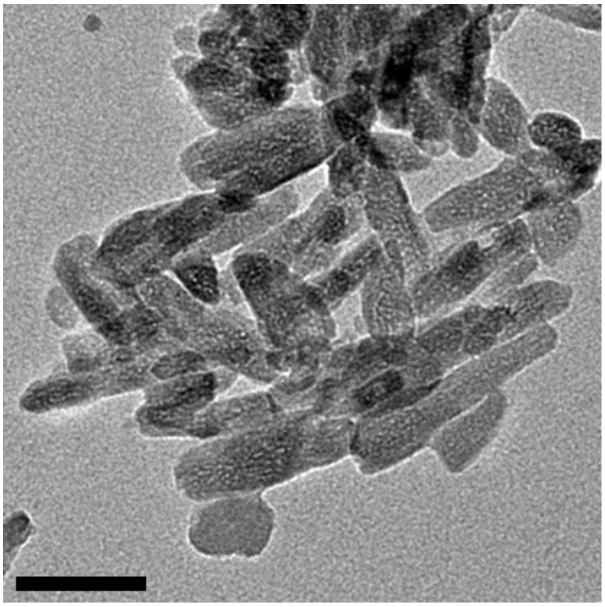

Figure S1. TEM images of CPNs (scale bar means 100 nm).

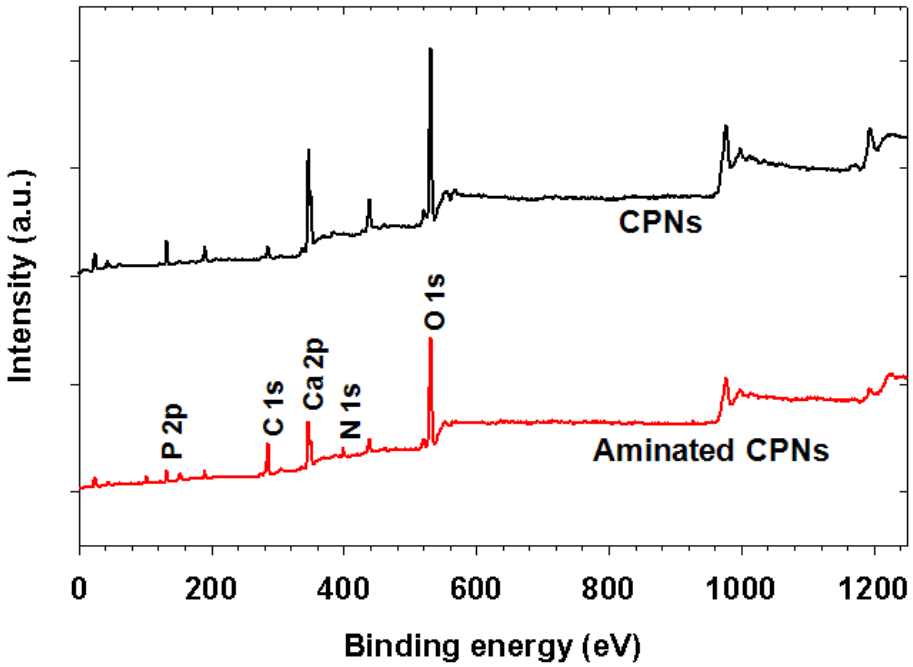

Figure S2. X-ray photoelectron spectroscopy for CPNs and aminated CPNs (CPNs-NH_2).

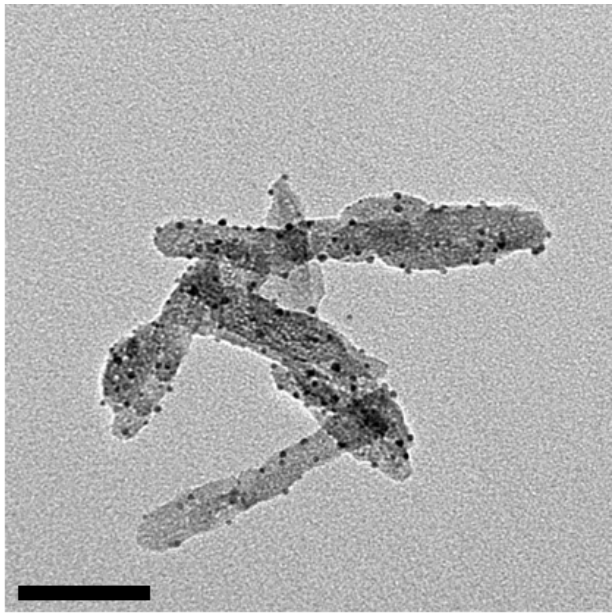

Figure S3. TEM images of CPNs-GNP (scale bar means 100 nm).

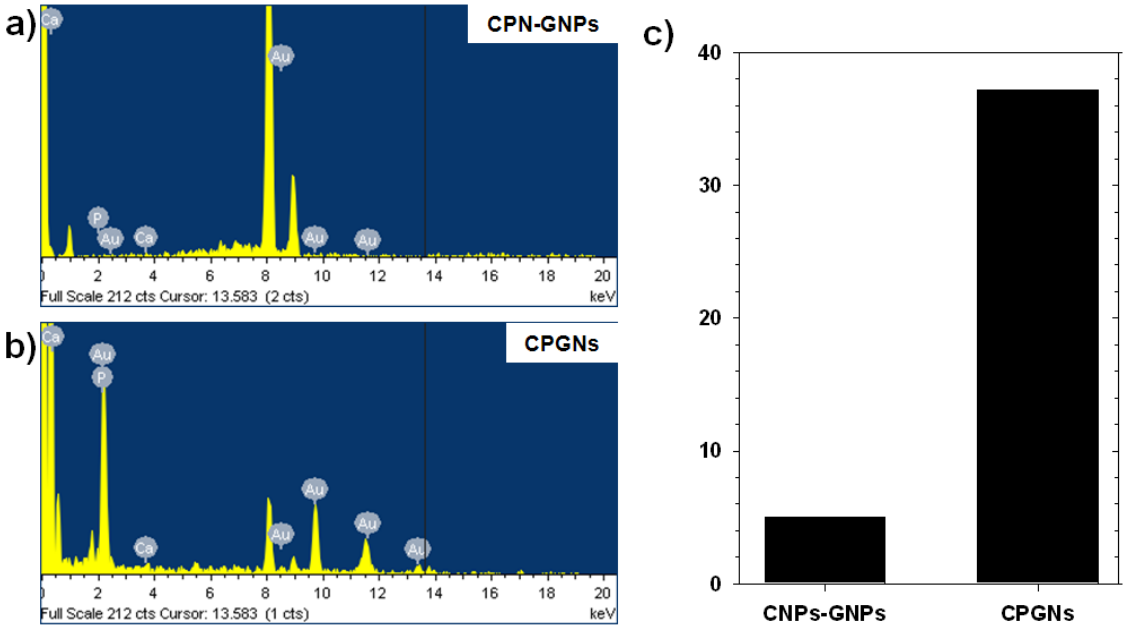

Figure S4. Energy-dispersive X-ray spectroscopy spectra of a) CPNs-GNP and b) CPGNs, and c) Au compositions of CNPs-GNPs and CPGNs, repectively.

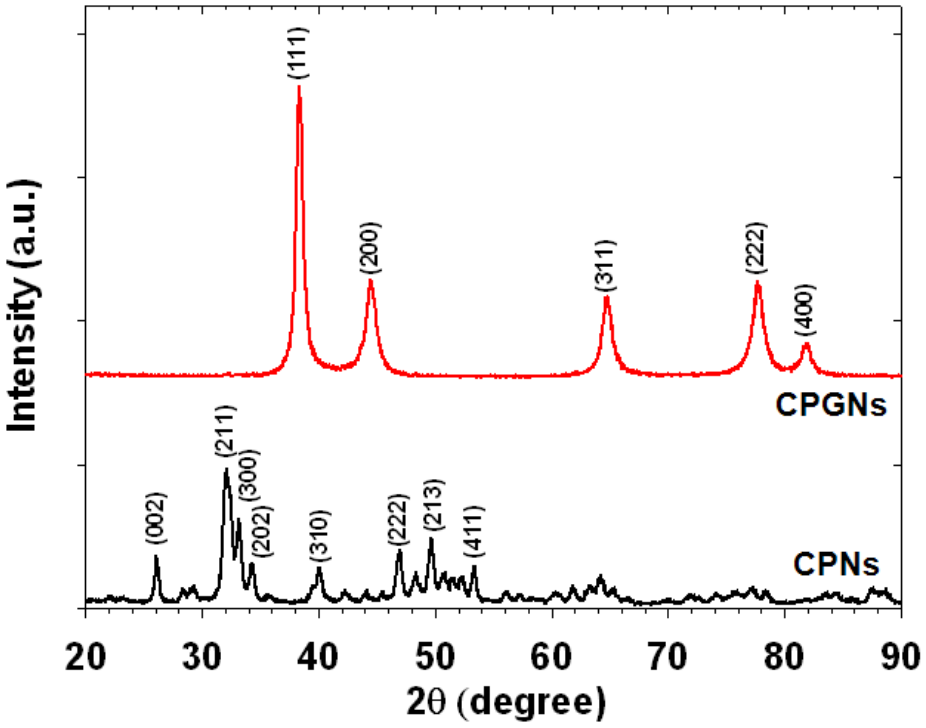

Figure S5. X-ray diffraction patterns of CPGNs and CPNs.

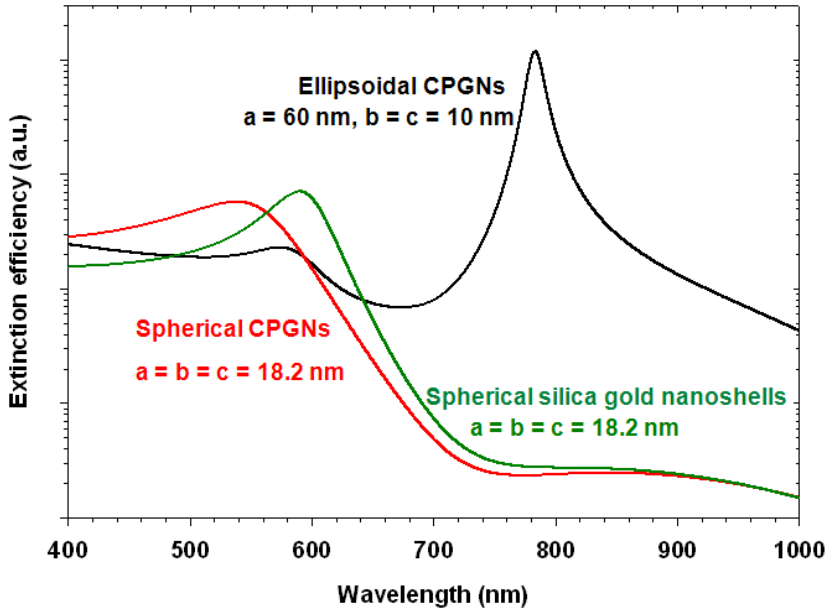

Figure S6. Comparison of the calculated extinction spectra for ellipsoidal CPGN, spherical CPGN and spherical silica-gold core-shell (gold thickness = 10 nm).

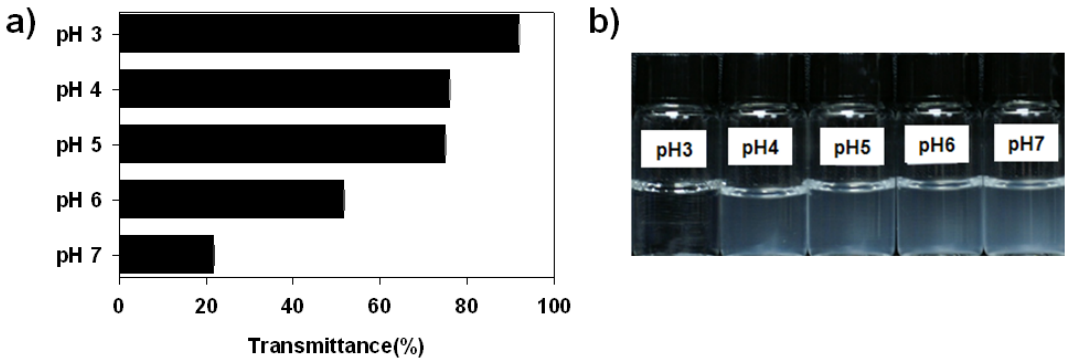

Figure S7. a) Transmittance of CPNs at various pH conditions to examine the potential for biodegradability. b) The photograph show the turbidities of CPN solutions according to the degree of degradation (pH 3 ~ 7).

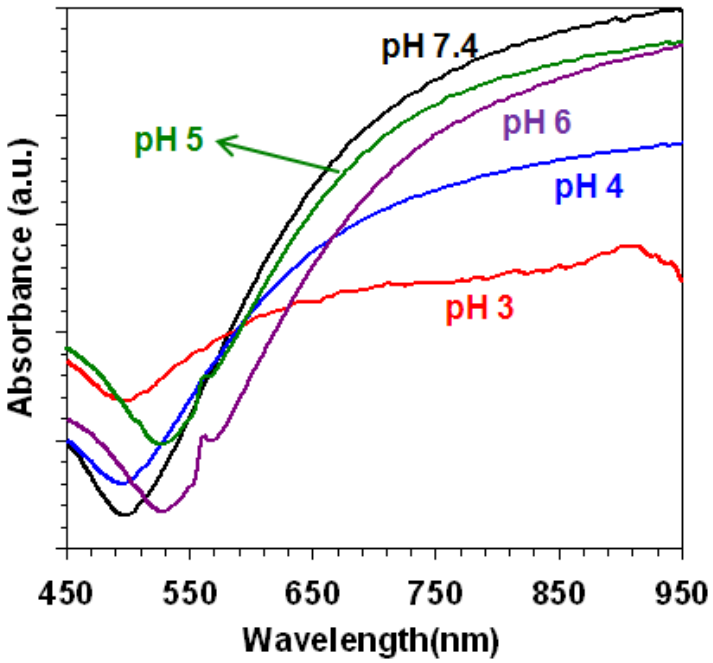

Figure S8. UV-Vis absorbance spectra of CPGNs at pH 3, 4, 5, 6 and 7.4 after 120 hours.

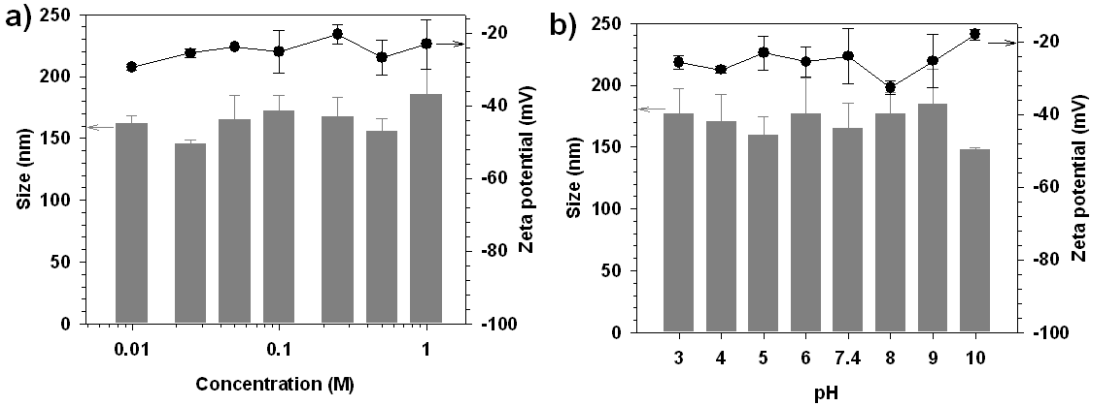

Figure S9. Particle size and zeta potential of ERB-CPGNs plotted against various (a) pH conditions and (b) NaCl concentrations.

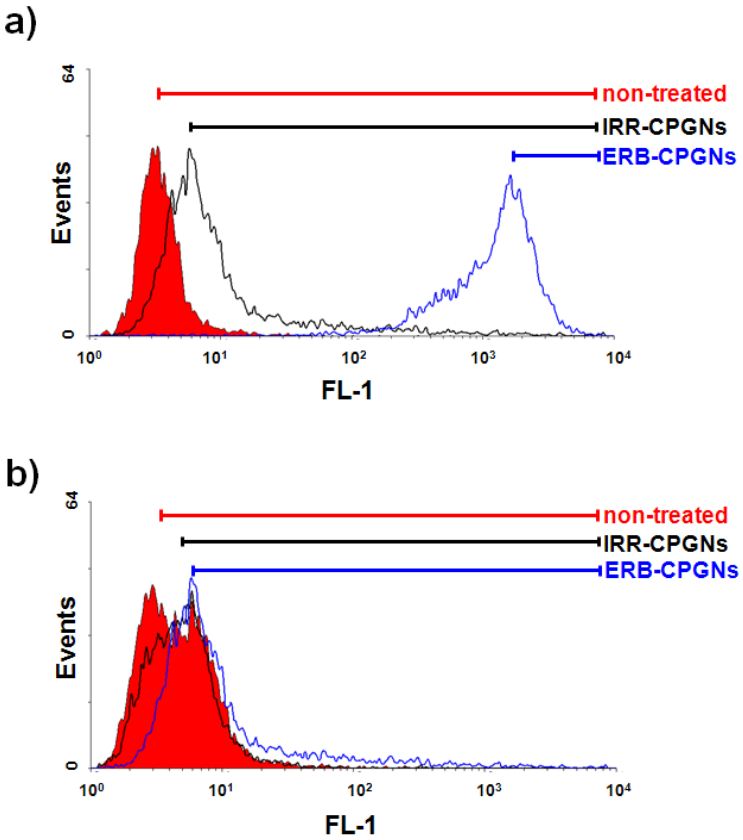

Figure S10. FACS analysis of a) A431 and b) MCF7 cells incubated with ERB-CPGNs and IRR-CPGNs, respectively.

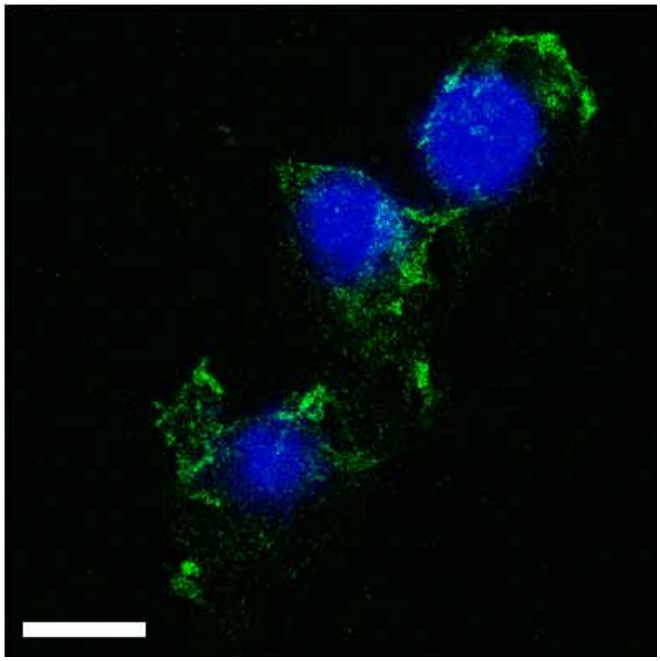

Figure S11. Confocal microscope image of A431 cells treated with ERB-CPGNs (scale bar means 5 μm).

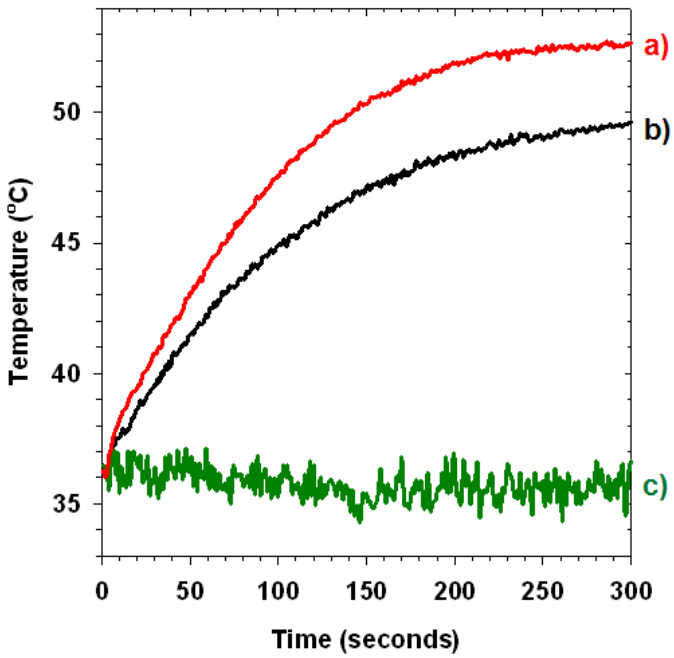

Figure S12. Temperature variations for incubation wells of a) only CPGNs solution, b) A431 cells treated with ERB-CPGNs and c) non-treated A431 cells after NIR laser irradiation (820 nm and 25 W/cm^2 for 5 minutes), respectively.

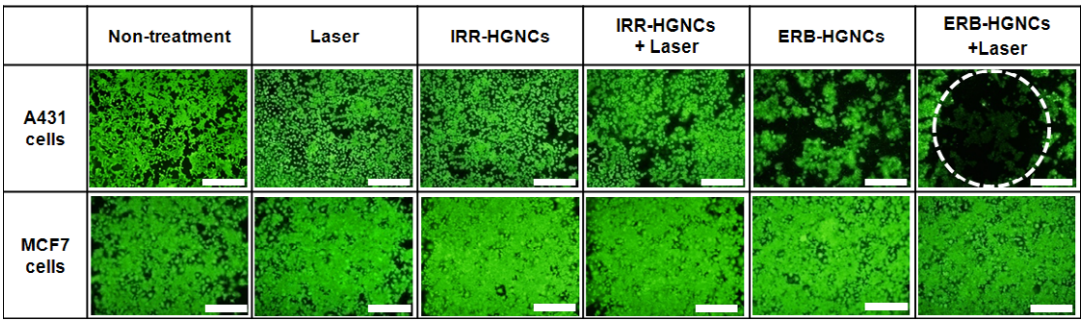

Figure S13. Fluorescence microscopic images of A431 or MCF7 cells stained with calcein AM for each after treatment; non-treatment, laser only, IRR-CPGNs, IRR-CPGNs + laser, ERB-CPGNs and ERB-CPGNs + laser, respectively (scale bar means 1 mm).

References

1. H. J. Lee, H. W. Choi, K. J. Kim and S. C. Lee, *Chem. Mater.*, 2006, **18**, 5111-5118.
2. X. Wang, A. Klocke, B. Mihailova, L. Tosheva and U. Bismayer, *J. Phys. Chem. B*, 2008, **112**, 8840-8848.
3. E. D. Palik, *Handbook of Optical Constants of Solids* Academic Press, 1991.